


SEPTEMBER 09 2025

Acoustic evidence of year-round sperm whale foraging, population structure, and sex-specific migration near Svalbard^{a)} **FREE**

Angela R. Szesciorka ; Manuel Bensi; Patrizia Giordano; Francesco Paladini de Mendoza; Aniello Russo; Giacomo Giorli



J. Acoust. Soc. Am. 158, 1921–1933 (2025)

<https://doi.org/10.1121/10.0039060>



Articles You May Be Interested In

Analysis of underwater acoustic data collected under sea ice during the Useful Arctic Knowledge 2021 cruise

Proc. Mtgs. Acoust. (July 2022)

Wind- and tidal driven ambient noise in seasonally ice-covered waters north of the Svalbard archipelago

JASA Express Lett. (August 2022)

Underwater vocal complexity of Arctic seal *Erignathus barbatus* in Kongsfjorden (Svalbard)

J. Acoust. Soc. Am. (November 2017)




COMSOL

Develop safe and reliable electronic devices

» See how simulation is used in the electronics industry

Acoustic evidence of year-round sperm whale foraging, population structure, and sex-specific migration near Svalbard^{a)}

Angela R. Szesciorka,¹  Manuel Bensi,² Patrizia Giordano,³ Francesco Paladini de Mendoza,⁴ Aniello Russo,¹ and Giacomo Giorli^{1,b)}

¹NATO Centre for Maritime Research and Experimentation, La Spezia 19126, Italy

²National Institute of Oceanography and Applied Geophysics, OGS, Trieste 34010, Italy

³Institute of Polar Sciences, National Research Council, Bologna 40129, Italy

⁴Institute of Polar Sciences, National Research Council, Messina 98122, Italy

ABSTRACT:

The Atlantification of the Arctic is driving a northward habitat shift of many cetaceans, including sperm whales (*Physeter macrocephalus*). As Arctic warming continues to decrease sea ice extent and contributes to the change in species distributions, it is crucial to study how the distribution patterns, habitat, and the demographic structure of sperm whale populations may continue to change. In this study, we assess the temporal presence of echolocating sperm whales on the continental slope southwest of the Svalbard archipelago and compare it with acoustic backscatter and temperature as a proxy for biomass. Size classes of echolocating whales were estimated using cepstral analysis. Echolocation rates were higher in summer and fall, suggesting a seasonality in the sperm whale presence; however, sperm whale clicks were present year-round and the acoustic backscatter and temperature were positively correlated with the recorded echolocation activity. The summer and fall size classes included a mix of large adult males, mid-sized sub-adult males and/or adult females, and social groups, which likely include immature animals and/or adult females and their offspring. We observed a shift to adult males in the winter, suggesting sex-specific partial migration at this site. © 2025 Acoustical Society of America. <https://doi.org/10.1121/10.0039060>

(Received 28 March 2025; revised 24 July 2025; accepted 7 August 2025; published online 9 September 2025)

[Editor: Lauren A. Freeman]

Pages: 1921–1933

I. INTRODUCTION

The Svalbard archipelago is located at the junction of the Greenland, Norwegian, and Barents Seas. This region is heavily influenced by the West Spitsbergen Current (WSC), a branch of the North Atlantic Current (Teigen *et al.*, 2011). While bounded by cold, coastal water from the East Spitsbergen Polar Current coming from the Barents Sea, the WSC transports warm, saline, nutrient rich water northward. The seasonal nutrient pulse from the WSC creates foraging hotspots for numerous marine mammals that inhabit or migrate to the Greenland and Barents Seas (Hamilton *et al.*, 2022). However, the WSC has undergone warming in the last two decades (Spielhagen *et al.*, 2011; Tverberg *et al.*, 2014; Lind *et al.*, 2018). Rapid warming and sea ice loss driven by climate change has then resulted in the expansion of warm, salty, nutrient-rich Atlantic Water even further northward causing the Atlantification of Arctic waters (Wassmann *et al.*, 2011; Barber *et al.*, 2015; Polyakov *et al.*, 2020).

Atlantification has begun to fundamentally alter the ecosystem, which has also caused the northward expansion of Atlantic marine mammals into the Arctic (Storrie *et al.*, 2018; Bengtsson *et al.*, 2022; Davis *et al.*, 2020; Nieukirk

et al., 2020) as well as their migrations. Humpback whale (*Megaptera novaeangliae*) abundance is increasing in south-east Greenland (Jansen *et al.*, 2016; Hansen *et al.*, 2019) and fin whales (*Balaenoptera physalus*) remain in Davis Strait until the end of December (Simon *et al.*, 2010). Blue whales (*Balaenoptera musculus*) are arriving to eastern Greenland one month earlier (Ahonen *et al.*, 2021) and killer whale (*Orcinus orca*) presence in Canadian Arctic waters is also increasing during the ice-free season (Lefort *et al.*, 2020; Garroway *et al.*, 2024).

The northernmost Atlantic distribution of sperm whales (*Physeter macrocephalus*) has historically been in the Davis Strait, as well as the Barents and Norwegian Seas (Berzin, 1972; Christensen *et al.*, 1992; Davidson, 2016; Evans, 1997; Madsen *et al.*, 2002; Weir *et al.*, 2001). However, sperm whales have been documented in Baffin Bay (75°N) off northwest Greenland (Frouin-Mouy *et al.*, 2017), where their presence may be increasing (Posdaljian *et al.*, 2022) and within the Arctic Circle (81°N), north of Barents Sea (Kovacs *et al.*, 2015; Vacquié-Garcia *et al.*, 2017; Storrie *et al.*, 2018; Pöyhönen *et al.*, 2024). The adult males typically migrate to forage in higher latitudes in the summer, while adult females with calves and juveniles remain in lower and mid-latitudes year-round (Best, 1979; Rice 1989; Connor *et al.*, 1998; Whitehead, 2003). A number of studies have documented sperm whale presence in the Greenland, Barents, and Norwegian Seas (e.g., Klinck *et al.*, 2012;

^{a)}This paper is part of a special issue on Climate Change: How the Sound of the Planet Reflects the Health of the Planet.

^{b)}Email: giacomo.giorli@cmre.nato.int

De Vreese *et al.*, 2018; Bengtsson *et al.*, 2022; Pöyhönen *et al.*, 2024). Pöyhönen *et al.* (2024) was the first to use passive acoustic monitoring (PAM) to assess the multi-year acoustic presence of sperm whales around the Svalbard Archipelago, with a focus on the High Arctic. However, if whales are pushing further north due to Atlantification, we hypothesized that the population trends in the lower Arctic waters would also change.

Sperm whales frequently dive to depths of 500–2000 m for up to 60–90 min (Teloni *et al.*, 2008; Irvine *et al.*, 2017; Watwood *et al.*, 2006), during which they emit constant clicks (Watkins, 1980) for echolocation (Goold and Jones, 1995; Møhl *et al.*, 2000; Jaquet *et al.*, 2001). These clicks are primarily used to locate mesopelagic squid (Kawakami, 1980; Rice, 1989; Santos *et al.*, 1999) but also to detect fish, particularly in higher latitudes (Clarke and MacLeod, 1976; Martin and Clarke, 1986; Kawakami, 1980; Rice, 1989). These highly directional, powerful echolocation clicks have a broadband frequency extending to 30 kHz (centroid frequency 15 kHz), source levels reaching 236 dB re 1 μ Pa at 1 m [root mean square (RMS)], and durations up to 100 ms (Møhl *et al.*, 2003). Variations in source level and click duration depend on click type and body size (Backus and Schevill, 1966; Gordon, 1991; Møhl *et al.*, 2003; Growcott *et al.*, 2011), with adult males producing more powerful clicks at a slower rate than adult females and juveniles (Goold and Jones, 1995; Solsona-Berga *et al.*, 2022).

Depending on the inter-click interval (ICI), clicks are classified as usual, slow, creaks, or codas (Gordon, 1987; Whitehead and Weilgart, 1991; Weilgart and Whitehead, 1988; Whitehead, 1993; Watkins and Schevill, 1977; Pavan *et al.*, 2000). Usual clicks are the most common echolocation signals used for navigation and foraging (ICI 0.5–2 s). Because sperm whales produce echolocation clicks frequently during foraging dives (Miller *et al.*, 2004; Watwood *et al.*, 2006; Giorli and Goetz, 2019), it makes them ideal candidates for detection using PAM. PAM is a cost-effective and non-invasive method for studying the distribution and behavior of acoustically active species, especially for species that performs long dive cycles. It enables long-term, year-round data collection in areas where other methods would be challenging and at times when polar night and poor weather would eliminate visual survey methods (Giorli and Pinkerton, 2019, 2023; Miller and Miller, 2018). Additionally, the repetitive nature of sperm whale clicks, with consistent temporal and frequency characteristics, makes them ideal for automated detection (Skarsoulis *et al.*, 2022; Ward *et al.*, 2012).

Finally, the structure of the sperm whale echolocation signals also allows the estimation of body length. Norris and Harvey (1972) hypothesized that the spermaceti organ plays a key role in sound production and that the multi-pulse structure (Backus and Schevill, 1966) of sperm whale echolocation clicks results from a single pulse bouncing between reflective air sacs at either end of the spermaceti organ. Thus, assuming the inter-pulse interval (IPI), which represents the two-way travel time in the spermaceti organ, is a constant property and an allometric relationship between

spermaceti organ length and body length (Nishiwaki *et al.*, 1963; Clarke, 1978), IPIs could be used to determine the body length of a sperm whale.

Understanding of the sound pathways within the spermaceti organ was further refined by Møhl *et al.* (1981) and Møhl (2001) as the “bent-horn model.” The updated hypothesis has been supported by a number of studies since then (Adler-Fenchel, 1980; Gordon, 1991; Møhl and Amundin, 1991; Madsen *et al.*, 2002; Møhl *et al.*, 2003; Zimmer *et al.*, 2005a; Zimmer *et al.*, 2005b), and the length equations developed by Gordon (1991) and Growcott *et al.* (2011) continue to be used in recent studies (Giorli and Goetz, 2020; Solsona-Berga *et al.*, 2022; Posdaljian *et al.*, 2024).

Here, we examine the multi-year presence of sperm whales southwest of the Svalbard Archipelago using two years (June 2022–July 2024) of PAM with automated click detection methods. Acoustic data were collected using a mooring deployed in the region, and we also assessed size classes and, for the first year of deployment, the relationship with acoustic backscatter and temperature from data collected at the same mooring.

II. METHODS

A. Data collection

Passive acoustic data were collected from an omnidirectional Autonomous Underwater Acoustic Data Logger (Loggerhead Instruments Inc., Sarasota, FL) mounted on a mooring named S1. S1 was developed and maintained by the National Research Council, Institute of Polar Sciences and the National Institute of Oceanography and Applied Geophysics (OGS) since June 2014. The acoustic recorders were first mounted on the S1 mooring during the Nordic Recognized Environmental Picture (NREP22) sea trial in June 2022. In the summer 2023, mooring S1 was serviced during the Arctic Climate Observatory (ACO23) research cruise, and finally re-deployed in July 2023. Both cruises were led by the North Atlantic Treaty Organization (NATO) Science and Technology Organization’s Centre for Maritime Research and Experimentation (CMRE).

Since 2014, the S1 mooring has been deployed at $\sim 76.44^\circ\text{N}$, 13.95°E (Fig. 1; supplementary material Fig. 1) at 1042 m depth. The location of the mooring was chosen because it lies at the convergence of Atlantic Water with dense waters from Storfjorden (Svalbard’s largest fjord) and shelf waters from the West Spitsbergen continental shelf (Bensi *et al.*, 2019; Bensi *et al.*, 2025). Thermohaline data were collected at various depths, from 480 m to the seafloor, via conductivity-temperature-depth measurements (CTD) (Sea-Bird Electronics, Bellevue, WA; models SBE16 and SBE37) and thermistors (model SBE56), with sampling time intervals from 15 min to 60 min. The data were checked for quality and compared with those of the vertical CTD casts carried out before each recovery and deployment of the mooring. The NREP22 hydrophone was located at a depth of 557 m, and the ACO23 hydrophone was located at a depth of 453 m. For both deployments, the sampling

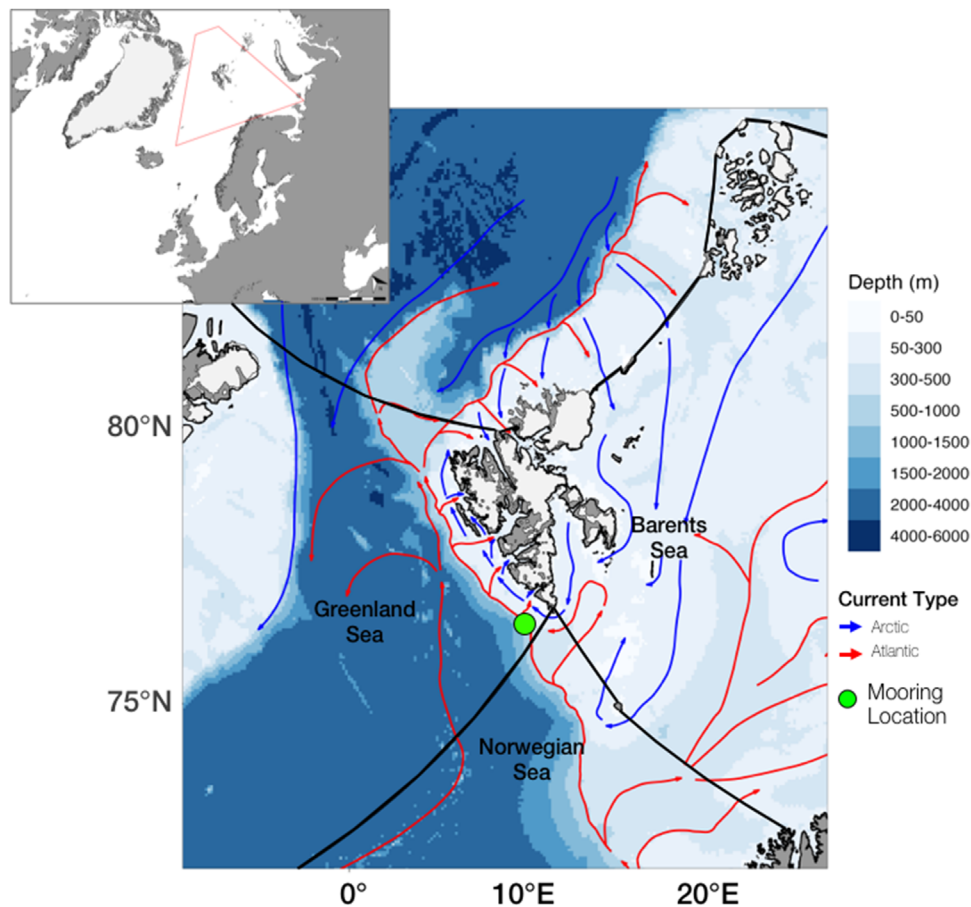


FIG. 1. Location of S1 mooring at the junction of the Greenland, Norwegian, and Barents seas. The green circle indicates the location of the S1 mooring. The red arrows indicate warm Atlantic water, and the blue arrows indicate cold Arctic water. International Hydrographic Organization Sea Areas were downloaded from <https://www.marinerregions.org/> (Flanders Marine Institute, 2018).

frequency was 96 000 Hz, the system sensitivity was -170 dB re $1 \text{ V}/\mu\text{Pa}$, gain was 2 dB re V/V, bit rate was 16-bit, and A-to-D converter zero-to-peak voltage was 1.0 V. The NREP22 hydrophone was operated on a duty cycle (Table I) recording 2 min every 15 min (resulting in four 2-min long .wav files per hour; 13.3% duty cycle). The ACO23 hydrophone was operated on a duty cycle (Table I) recording 10 min every hour (resulting in one 10-min long .wav file per hour; 20% duty cycle).

All figures were made in R (R Core Team, 2024) with “sf” (Pebesma, 2018; Bivand, 2023), “ggplot2” (Wickham, 2016), “ggOceanMaps” (Vihtakari, 2024), and “ggspatial” (Dunnington, 2023).

B. Sperm whale click detection

Sperm whale clicks were detected using a custom algorithm in Matlab (MathWorks, Inc., Natick, MA) with the

approach described by Giorli and Goetz (2019, 2020) and Giorli and Pinkerton (2023). Briefly, the acoustic data were bandpass filtered between 4 and 30 kHz. An adaptive threshold of 6 dB above average ambient noise was used to identify clicks, which were grouped into click trains if the ICI was less than 3 s and if there were at least three clicks per click train. At this stage, our main scope was to isolate click trains from any sperm whale. The probability of each click train being produced by a sperm whale was computed by dividing the number of clicks that meet the criteria for peak frequency (4–15 kHz), ICI (0.25–2 s), and click duration (500–1200 μs) by the total number of clicks in the click train. The duration of each echolocation click was measured as the time interval between the 5th and 95th percentiles of the energy obtained by integrating the square pressure over a 2 ms window around the signal. A window of 2 ms long was chosen to capture the entire echolocation signal (Møhl et al., 2003). The peak frequency was measured as the

TABLE I. Mooring deployment and hydrophone sampling information.

Cruise	Hydrophone depth (m)	Deployment time	Recovery time	Duty cycle (on/off; min)	Sample rate (kHz)	A/D converter (0 to peak; V)	Bit rate	Gain (dB)	Sensitivity (dB re $1 \text{ V } \mu\text{Pa}^{-1}$)
NREP22	557	2022/6/25 13:30:00	2023/6/22 08:00:00	2/13	96	1.0	16	2.05	-170
ACO23	453	2023/7/7 11:18:00	2024/7/4 09:00:00	10/50	96	1.0	16	2.0	-170

frequency corresponding to the peak of the spectrum of the 2 ms signal window. ICIs were computed as the time interval between the peak pressure between two consecutive clicks. A click train was considered to be produced by a sperm whale if the probability was greater than 0.5.

Peak frequency, ICI, and click duration ranges were initially chosen based on the literature (Zimmer *et al.*, 2003; Zimmer *et al.*, 2005a; Giorli and Goetz, 2019, 2020). The detector performance was determined using a receiver-operator characteristic (ROC) approach. A series of 11 detector trials were tested using a training dataset created from .wav files collected both in NREP22 and ACO23. The training dataset consisted of 65 files (five files per month) that contained only sperm whale echolocation clicks and 65 files (five files per month) that did not contain sperm whale echolocation clicks. Performance was assessed across the 11 different trials varying clicks parameters, percent probability, and the adaptive threshold dB value above average ambient noise (supplementary material Fig. 2). The highest performing combination was then used to analyze the full dataset. The parameters that returned the best detector performance were (1) peak frequency between 4 and 15 kHz; (2) ICI between 0.25 and 2 s; and (3) click duration between 500 and 1200 μ s, probability of 0.5, detection threshold 6 dB above ambient noise. Performance from the full data set was assessed using 100 randomly chosen files per year.

C. Sperm whale size estimates

The body length of detected sperm whales was estimated using the methodology described by Teloni *et al.* (2007), Giorli and Goetz (2019), and Caruso *et al.* (2015). Briefly, stable IPIs were identified averaging the cepstra obtained from each echolocation click in separate click trains (Zimmer *et al.*, 2005b). Only click trains with more than 50 clicks were used (Giorli and Goetz, 2019; Caruso *et al.*, 2015). The cepstra from each echolocation signal in a click train were averaged to obtain a mean cepstrum, and the mean IPI was identified as the maximum gainitude between a quefrequency of 2 and 13 ms of the mean cepstrum (Goold *et al.*, 1996; Giorli and Goetz, 2019; Caruso *et al.*, 2015). This approach assumes the echolocation signals in each click train are produced by the same individual. After visual inspection, any average cepstrum without a clear peak in gainitude was discarded (supplementary material Fig. 3). To reduce the chances of measuring the same individual multiple times, an autocorrelation filter was applied to excluded IPI measurements if (1) they occurred within two hours of a previous measurement, and (2) if they differed by less than 0.3 ms from the previous measurement (Böttcher *et al.*, 2018). However, this approach does not avoid counting the same animal multiple times if it had to visit the area in different days of the month. Potential outliers were removed if the value was 1.5 interquartile ranges above the upper quartile or below the lower quartile (Schwertman *et al.*, 2004). The measured mean IPI was then used to estimate the size of the sperm whale producing the

click train using the equations proposed by Gordon (1991) and Growcott *et al.* (2011). Gordon’s formula is well suited for measurements of individuals < 11 m (\sim 4 ms IPI); while Growcott’s equation better fits the measurement of larger individuals (IPI > 4 ms) (Caruso *et al.*, 2015). Combining the IPIs with the appropriate size formula, we then broadly categorized size classes as defined by Caruso *et al.* (2015): >12 m as adult males (hereafter “Adult Males”), 9–12 m as mid-sized adult females and/or sub-adult males (hereafter “Mid-Sized”), and <9 m as immature animals and/or adult females and their offspring (hereafter “Social Groups”).

D. Backscatter intensity estimation

During the NREP22 deployment, an acoustic Doppler current profiler (ADCP 150 kHz; Teledyne RD Instruments, Poway, CA) was mounted on mooring S1 at 488 m with a four-beam (20°) downward-looking configuration. During the ACO23 cruise, the ADCP was upward-looking. We only included the first year of ADCP data since the downward-looking configuration is more relevant to collect data on deep biomass that constitute prey for sperm whales. In fact, sperm whales are deep-diving predators that forage during the bottom phase of their dives (Watwood *et al.*, 2006). Despite the lack of direct measurements of zooplankton abundance, the ADCP backscatter signal has been demonstrated to provide qualitative insights into the composition and dynamic of the zooplankton community (Ursella *et al.*, 2018; Guerra *et al.*, 2019; Liu *et al.*, 2022), particularly in open-ocean settings where contributions from suspended sediments are negligible. To evaluate the particle concentration in the water column resulting from the contribution of sediment and zooplankton (Reichel and Nachtnebel, 1994), we estimated the acoustic backscatter strength (Sv) for each depth cell from the broadband ADCPs, starting from the echo amplitude signal (E). Many different mathematical methods exist to estimate the backscatter. While Deines (1999) is the most frequently referenced, Mullison (2017) better resolves signal and noise in a low backscatter environment with low concentrations of suspended matter, such as in pelagic environments. The backscatter (BS) equation determined by Mullison (2017), including signal (S) and noise (N), plus terms that depend on the ADCP, oceanographic conditions, and sampling strategy, is

$$BS = C + 10 \log((T_x + 237.16) R^2) - L_{b\text{dm}} - P_{\text{dbw}} + 2\alpha R + 10 \log(10^{Kc(E-E_r)/10} - 1), \quad (1)$$

where E (in counts) is the returned signal strength indicator (RSSI) amplitude, reported by the ADCP for each bin along each beam; E_r is the reference noise floor RSSI amplitude, a constant for each beam of a given ADCP and is available from factory parameters calibration; K_c is a conversion factor of the amplitude counts reported by the ADCP receiver circuitry to decibels (dB); and C (−153.3, for this study) is an instrumental constant. Values for E_r , K_c , and C were

provided by the manufacturer. L_{dbm} (34.32, for this study) is the 10 log (transmit pulse length, L) and P_{dbw} (15, for this study) is the 10 log (transmit power, W), which is provided by the manufacturer. T_x is real-time temperature ($^{\circ}C$) of the transducer, R is the slant range, which is the range to the relevant scattering layer along the beam and is calculated by

$$R = \left[(B + (L + D)/2 + (N - 1)D + (D/4)) / \cos \theta \right] c / c_1, \tag{2}$$

where B (29.47, for this study) is blank after transmit, D (8, for this study) is the depth cell length, N is the depth cell number of the scattering layer being measured, θ (20° , for this study) is the beam angle, c is the average sound speed from the transducer to the range cell, and c_1 is the speed of sound used by the instrument.

Transmission loss along the water column depends on absorption of acoustic energy by the sea water. The absorption for each range cell, $\alpha_n = 2\alpha D / \cos(\theta)$ where α is the absorption coefficient at that depth. The value of $2\alpha R$ is determined by

$$2\alpha R = \left(\frac{2\alpha\beta}{\cos \theta} \right) + \sum_{n=1}^b \alpha'^n, \tag{3}$$

where α' is the absorption at the profiler and b is the range cell number. The absorption coefficient is calculated by the algorithms from [Stevens \(2022\)](#), which used the [Fisher and Simmons \(1977\)](#) and [Ainslie and McCollm \(1998\)](#) equations based on viscous absorption generated by particle motion and absorption by specific chemicals reported in [Kinsler et al. \(2000\)](#).

The oceanographic parameters of salinity and temperature used for the determination of the coefficient α are retrieved by the measurements conducted on the mooring by the SBE probe at 506 and 597 m depth. To ensure the accuracy of backscatter measures, the ADCP tilt data were quality controlled by verifying that the tilt angle did not exceed 20° , which is the critical threshold for maintaining data integrity and correct slant range calculation, which is a fundamental term in the backscatter formula.

III. RESULTS

A. Click detection performance

The trials with the test dataset (Table II), which included 65 files with sperm whale clicks and 65 files without sperm whale clicks, resulted in a 98.5% true positive

rate, 100% true negative rate, 0% false positive rate, and 1.5% false negative rate. Precision (true positive relative to total number of true and false positives) was 100%. Recall (true positive relative to the total number of true positives and false negatives) was 98.5%. The F-score ([Powers, 2020](#); [Davis and Goadrich, 2006](#)), a measure of the overall accuracy, was 99%.

The detector identified 21 199 sperm whale echolocation click trains in 8514 files from the first year of data (NREP22). The assessment of the performance on the real dataset of NREP22 resulted in a 100% true positive rate, a 98% true negative rate, 0% false positive rate, and a 2% false negative rate. Precision (true positive relative to total number of true and false positives) was 100%. Recall (true positive relative to the total number of true positives and false negatives) was 98%. The F-score was 99%.

The detector identified 25 355 sperm whale echolocation click trains in 3282 files from the second year of data (ACO23). The assessment of the performance on the real dataset of ACO23 resulted in a 96% true positive rate, a 100% true negative rate, 4% false positive rate, and a 0% false negative rate. Precision (true positive relative to total number of true and false positives) was 96%. Recall (true positive relative to the total number of true positives and false negatives) was 100%. The F1 beta score (accuracy) was 98%.

B. Temporal trends

Data collection during NREP22 resulted in more than 1158 effort hours from 34 730 2-min files spanning June 2022 to June 2023. Data collection during ACO23 resulted in more than 1449 effort hours from 8738 10-min files spanning July 2023 to July 2024. Effort for both years was roughly equal and consistent across months (13% and 16%, respectively; Table III); however, effort was reduced during deployment and recovery months.

Sperm whale echolocation clicks were detected month- and year-round in both deployment years (Table III; Fig. 2). Sperm whale echolocation clicks were only absent for 48 non-continuous days out of 363 days of effort in the first year and for 53 non-continuous days out of 364 days of effort during the second year. Despite the year-round presence, seasonal trends were evident. The summer and fall months had the highest number of sperm whale echolocation click detections, with at least one month each summer exceeding a 60% presence (which we calculated as the number of hours with clicks compared to number of effort hours

TABLE II. Performance metrics (i.e., true positive, true negative, false positive, and false negative) for the test data set, which included 65 files with clicks and 65 without clicks that were manually validated and the full dataset for each year, of which 100 randomly chosen files were manually validated.

	Test dataset ($n = 130$ files)		NREP22 dataset ($n = 100$ files)		ACO23 dataset ($n = 100$ files)	
	Positive	Negative	Positive	Negative	Positive	Negative
Positive	64	1	50	0	48	2
Negative	0	65	1	49	0	50

TABLE III. Summary of monthly sperm whale echolocation click detections, including total files, recording hours, click hours, presence ratio (hours with clicks vs effort hours), and percent effort. The black line indicates the month in which the mooring was refurbished.

Year	Month	Total files	Recording hours	Click hours	Presence ratio	Percent effort
2022	6	522	131	68	0.52	2.4
2022	7	2976	744	531	0.71	13.3
2022	8	2976	744	360	0.48	13.3
2022	9	2880	720	309	0.43	13.3
2022	10	2976	744	427	0.57	13.3
2022	11	2880	720	439	0.61	13.3
2022	12	2976	744	347	0.47	13.3
2023	1	2976	744	287	0.39	13.3
2023	2	2688	672	57	0.08	13.3
2023	3	2976	744	47	0.06	13.3
2023	4	2880	720	80	0.11	13.3
2023	5	2976	744	320	0.43	13.3
2023	6	2048	512	255	0.50	9.5
2023	7	590	589	495	0.84	13.2
2023	8	744	743	408	0.55	16.6
2023	9	720	719	252	0.35	16.6
2023	10	744	743	319	0.43	16.6
2023	11	720	719	437	0.61	16.6
2023	12	744	743	235	0.32	16.6
2024	1	744	743	191	0.26	16.6
2024	2	696	695	62	0.09	16.6
2024	3	744	743	126	0.17	16.6
2024	4	720	719	115	0.16	16.6
2024	5	744	743	167	0.22	16.6
2024	6	720	719	388	0.54	16.6
2024	7	80	80	71	0.89	1.8

that month). Their presence decreased in winter, dropping below 10% by February, and then began increasing again slightly in the spring. Although there were more detections in most months during the first year of data collection, both years displayed the same overall seasonal pattern.

C. Size trends

The algorithm used to identify stable IPIs from the cepstra of each echolocation signal for size estimation resulted in 1839 click trains from NREP22 and 3718 click trains

from ACO23. The manual validation removed 1309 and 2916 click trains, respectively, resulting in 530 click trains and 757 click trains retained for further analysis. The auto-correlation filter removed 157 and 349, respectively, resulting in 373 click trains and 408 click trains retained. The final outlier filter removed 14 and 53, respectively, resulting in 359 click trains and 355 click trains retained. While the numbers retained for final analysis were small (and thus a limitation of this study), we were able to estimate sperm whale body lengths for each month with recording effort. The result was a mix of Adult Males, Mid-Sized animals (i.e., sub-adult males and/or adult females), and Social Groups (i.e., immature animals and/or adult females and their offspring). Adult males dominated throughout the time series; however, some seasonality was evident, with a greater mix of size classes in the summer, followed by a shift toward adult males in the winter (Fig. 3).

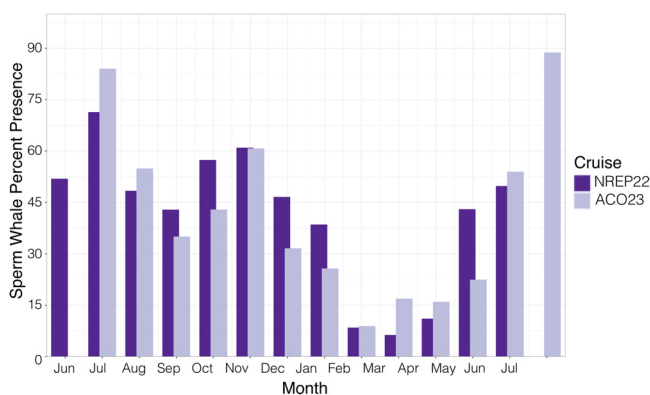


FIG. 2. Monthly sperm whale percent presence, calculated as number of hours with clicks compared to number of effort hours per month. Dark purple represents clicks detected from NREP22 (June 2022–June 2023) and light purple represents clicks detected from ACO23 (July 2023–July 2024).

D. Acoustic backscatter, temperature variability, and sperm whale presence

Temperature in the water column showed a seasonal pattern in the layer between 480 m and 600 m depth. Overall, the temperature fluctuates between -0.9°C and 4.0°C , with values $>2.0^{\circ}\text{C}$ related to the vertical shifts of the Atlantic Water from the upper layer to the deep one (Fig. 4). The highest values were recorded in November–December 2022 and in February 2023, the lowest in April–May 2023.

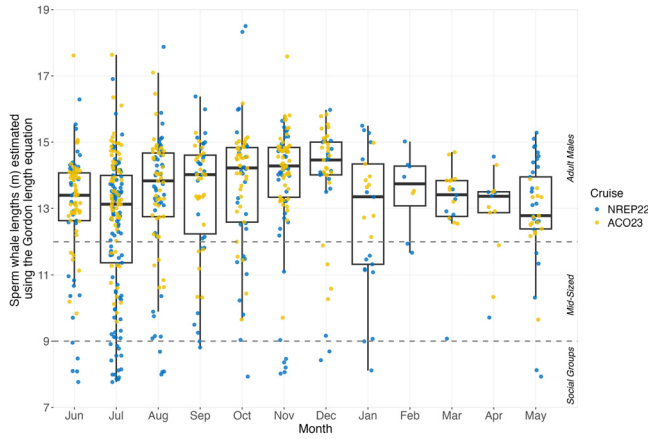


FIG. 3. Ranges of monthly sperm whale size estimates. Blue circles represent sizes estimated from clicks from NREP22 (June 2022–June 2023), and yellow circles represent sizes estimated from clicks from ACO23 (July 2023–July 2024). Dashed lines represent size classes with >12 m as Adult Males, 9–12 m as Mid-Sized adults (sub-adult males and/or adult females), and <9 m as Social Groups (immature animals and/or adult females and their offspring). Box and whisker plots represent combined median, upper (75th percentile or Q3) and lower (25th percentile or Q1) quartiles, and range (minimum and maximum) values.

Although somewhat driven by the low in April, temperatures at 500 m showed a linear, but non-significant, relationship with monthly sperm whale presence [$p = 0.10$, $R^2 = 0.25$; Fig. 5(A)], with higher sperm whale presence when water temperatures were warmer. The largest peak in backscatter intensity occurred in November and December; however, there were also pulses in the summer and spring. There was a low correlation between monthly sperm whale presence and mean monthly acoustic backscatter for all depth-intervals below 630 m (all $p < 0.05$). Backscatter intensity at

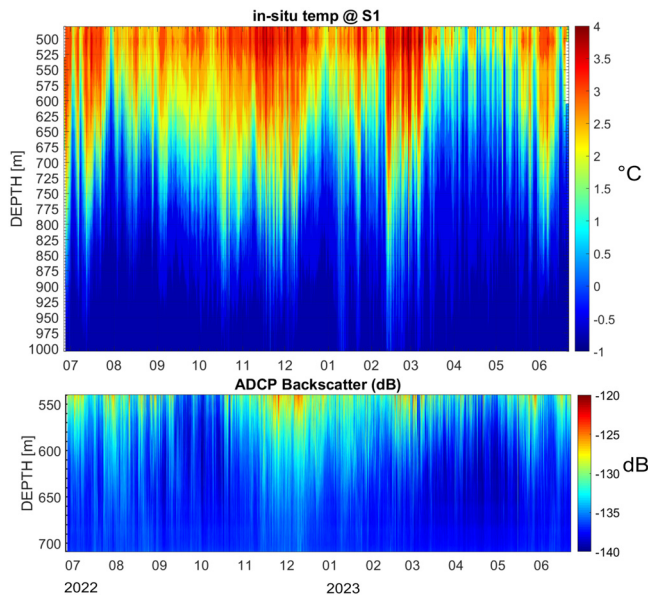


FIG. 4. (Upper panel) *In situ* temperature ($^{\circ}\text{C}$) from the mooring S1. (Lower panel) Acoustic backscatter intensity (dB) estimated from the downward-facing ADCP. Data cover the period from June 2022 until June 2023.

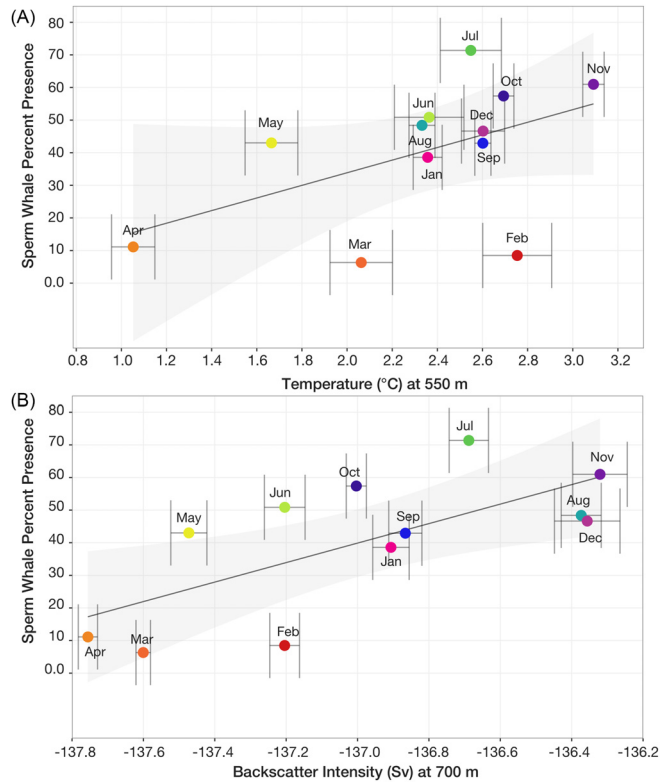


FIG. 5. Relationship between monthly sperm whale presence and (A) temperature ($^{\circ}\text{C}$) at 550 m and (B) backscatter intensity (Sv) at 700 m collected during NREP22 (June 2022–June 2023). Standard error bars are included for the monthly calculations of temperature and backscatter intensity.

700 m depth showed the greatest correlation with monthly sperm whale presence [$p = 0.1$, $R^2 = 0.48$; Fig. 5(B)]. Spring exhibited some of the lower intensity values, while summer, fall, and winter months fluctuated between moderate and higher intensity. The greatest intensity (-136.7 dB) corresponded to the highest percent of sperm whale presence in July (71%).

IV. DISCUSSION

The presence of sperm whales in Greenland, Barents, and Norwegian Seas is well known from visual survey (Christensen *et al.*, 1992; Øien, 2009; Storrie *et al.*, 2018; Bengtsson *et al.*, 2022), tag (Hamilton *et al.*, 2022), and PAM data (De Vreese *et al.*, 2018; Pöyhönen *et al.*, 2024). Similar to previous PAM studies, we found seasonality in the number of click hours per month, with greater presence in summer through fall and reduced presence in winter through spring. The WSC and the inflow of Atlantic water also show considerable seasonal fluctuations and tend to be stronger in winter and weaker in summer (Long *et al.*, 2024). However, the 1-year data from S1 show that in the intermediate layer, the highest temperatures were recorded in November–December 2022 and February 2023, and the lowest in April–May 2023. Such variability is strongly related to atmospheric disturbances that stimulate internal waves propagation (Bensi *et al.*, 2019). Our study also detected sperm whale clicks each month across the two-year

study period. This is not completely surprising as male sperm whales are wide-ranging nomads, capable of traveling at least 5000 km per year across ocean basins (Mizroch and Rice, 2013). However, to our knowledge, no other study has detected sperm whales year-round near Svalbard.

Pöyhönen *et al.* (2024) did not find year-round presence in their 10-year study; however, their hydrophones were deployed north of 78°, which would be at the higher end of sperm whale extent. That being said, they did detect whales in January at their northernmost site (81°N). Although visual sightings reported by De Vreese *et al.* (2018) in the Greenland Sea were not year-round, the presence of sperm whales in some winter and spring months also hint at a likely year-round presence. Off northern Norway, Rødland and Bjørge (2015) also reported winter sightings of sperm whales by local fishers and whale watching companies. Elsewhere, sperm whales have recently been documented year-round in the Gulf of Alaska and off Central California (Oestreich *et al.*, 2024; Posdaljian *et al.*, 2024).

Our findings also suggested a range of size classes, including adult males, mid-sized adult females and/or sub-adult males, and social groups including immature animals and/or adult females and their offspring. These size classes were well represented in the summer and fall, but shifted to almost entirely large adult males in the winter. In July, we observed the appearance of mid-sized immature males and/or adult females and social groups composed of immature animals and/or adult females and their offspring returning to high latitudes and an increase in foraging-related activities across the size classes. Similar size classes have also been documented in higher latitude sub-Arctic waters of the Gulf of Alaska (Posdaljian *et al.*, 2024; Oestreich *et al.*, 2024) and temperate waters off central California (Oestreich *et al.*, 2024). Despite the year-round presence of sperm whales in the Gulf of Alaska and off central California, Oestreich *et al.* (2024) found opposite seasonality at individual sites in the Gulf of Alaska and off central California and no temporal change in size classes, which their movement simulations suggested were due to resource-driven seasonal migration. However, Posdaljian *et al.* (2024) found seasonality among three equivalent size classes in the Gulf of Alaska across five recording sites. Although our study also only included one mooring location, the persistent presence of predominantly adult males from winter through spring suggests sex-specific partial migration at this site. Deploying additional hydrophones in nearby regions would help further investigate this hypothesis.

Questions remain about the number of animals present off southwest Svalbard, especially in winter, as well as their individual residence time in the region. In the Northern Hemisphere, sperm whales mate between January and August, peaking March–June (Rice, 1989), which may explain the lower sperm whale presence in winter through spring despite the increased backscatter intensity. It is possible whales detected in the summer either remained or returned after moving between groups of females while searching for receptive partners (Whitehead, 1993). Mature

males migrate to lower latitude breeding areas for a short period of time, only remaining with specific females for days to a week (Whitehead, 1993; Coakes and Whitehead, 2004; Gero *et al.*, 2014; Eguiguren *et al.*, 2023). Most males also do not begin mating until they are in their 20s (Best, 1979; Best *et al.*, 1984). Thus, it is possible some of the larger males remaining behind have not yet reached socio-sexual maturity (Eguiguren *et al.*, 2023) and therefore spend winter at higher latitudes eating and growing. Whether they are remaining year-round or returning after attempted or successful mating, foraging throughout the year allows males to grow bigger, which will allow them to compete for territories or females (Whitehead, 1994).

It is thought that sperm whale diet in high latitude North Atlantic consists of cephalopods and mesopelagic and bathypelagic fish (Øynes, 1957; Christensen, 1980; Bjørke, 2001), with males consuming a greater range and larger prey than females (Best, 1979; Clarke, 1980; Clarke *et al.*, 1988; Rice, 1989; Clarke *et al.*, 1993). The sperm whale habitat model by Storrie *et al.* (2018), based on visual sightings around Svalbard, suggested suitable areas in deeper waters along the continental slope, consistent with their known use of deep-water areas associated with their cephalopod prey throughout their range (Weir *et al.*, 2001). Their presence near the mooring site on the continental slope suggests that sperm whales feed on deep sea prey in this region. Additionally, the relationship with temperature and backscatter at the deeper sampling intervals also suggests that sperm whales were likely feeding on deep-sea pelagic species, potentially Atlantic species whose northward expansion (Snoeijs-Leijonmalm *et al.*, 2022) may have sustained their year-round presence at the site.

Animals presumably migrating to lower latitudes in the winter may include “bachelor schools,” groups of males that form long-term associations and forage in close proximity (Kobayashi *et al.*, 2020). They may also include females and mixed groups whose spatial and temporal distribution (Best *et al.*, 1984) in this region remain poorly understood. Early hypotheses on sperm whale distribution were that only males were found at higher latitudes (Ohsumi, 1966; Best, 1979) with the oldest and largest at the highest latitudes (Whitehead, 2018). Adult male sperm whales have long been documented along the continental slope from northern Norway to Svalbard (Øien, 2009). Adult females and juveniles are already known to nomadically travel up to 35 000 km in tropical or temperate waters (Whitehead, 2003). Females have also been increasingly observed at higher latitudes (Fearnbach *et al.*, 2012; O’Callaghan *et al.*, 2024); however, visual surveys have yet to report female sperm whales off Svalbard.

Sea ice has historically constrained the northernmost distribution of sperm whales, as they typically avoid ice-covered areas (Seger and Miksis-Olds, 2020; Posdaljian *et al.*, 2022). However, rapid warming (Rantanen *et al.*, 2022) has allowed sub-Arctic cetaceans to expand their northward extent further into the Arctic. Increased presence and expanded northward migratory routes have already been

observed in Baffin Bay, an area experiencing sea ice loss and longer open water seasons (Posdaljian *et al.*, 2022; Davidson *et al.*, 2023). With sperm whales being detected in the high Arctic (Kovacs *et al.*, 2015; Vacqu -Garcia *et al.*, 2017; Storrie *et al.*, 2018; P yh nen *et al.*, 2024) and the ongoing Atlantification of Arctic waters, other demographic groups may also be expanding their migratory routes northward, potentially taking advantage of shifts in prey distributions or new prey assemblages. The Atlantic Water intrusions detected on the deep sea mooring S1 (Fig. 5) are strongly related to seasonal and long-term changes in the WSC Arctic inflow. They are also signals of nutrient changes both at the surface and in the water column that could create favorable prey conditions for sperm whales in the region.

For size estimation, Adler-Fenchel (1980) found that ~11% of the clicks met the criteria for their analysis. In our study, we went from 5557 size estimates to 714 size estimates after applying our error reduction methods, which is roughly 13% of the total number of clicks originally detected. While the remaining size detections allowed us to assign size classes for each month of effort, they certainly do not represent the entire potential size class distribution in the study area. Future analysis could include the method described by Solsona-Berga *et al.* (2022), which uses the ICI (i.e., time between pulse trains) as a proxy for sperm whale body size and sex. Additionally, we cannot determine whether the smaller animals are females or males.

Finally, there are some limitations in using acoustic backscatter as a proxy for biomass, especially in such a localized area around a single mooring. While previous studies have found relationships between sperm whales and phytoplankton biomass, the correlations are weak at finer scales (Jaquet, 1996) suggesting other data on oceanography, environment, or prey may better explain the distribution of sperm whales on their foraging grounds.

V. CONCLUSIONS

Our study detected sperm whale echolocation clicks year-round with peaks in summer and fall. The summer and fall size classes included adult males, mid-sized adult females and/or sub-adult males, and social groups including immature animals and/or adult females and their offspring. This shifted to mainly adult males in winter, suggesting sex-specific partial migration. There were low positive correlations between echolocation click hours and temperature and acoustic backscatter, which may partially explain their year-round presence. This year round-presence corroborates other findings that sperm whales are shifting their northern extent into higher latitudes. However, many questions remain about the number, sex, and individual residence patterns of sperm whales off southwest Svalbard. Additional mooring locations, visual surveys, or tag data would help clarify how many sperm whales spend winter in this region and whether they remain year-round or return after visiting the breeding grounds. Echolocation clicks confirm that the whales are foraging along the continental slope, where deep-sea squid are

typically found, and their relationship with mean monthly acoustic backscatter further illuminated this and the importance of year-round foraging in the Arctic. As climate change continues to warm the Arctic, it remains uncertain how the distribution patterns and structure of sperm whale habitats may continue to change. Long-term monitoring is needed to understand the changing structure of sperm whale habitats, prey fields, and distributions for this far-ranging species.

SUPPLEMENTARY MATERIAL

See the [supplementary material](#) for a schematic representation of the mooring deployed for this study ([supplementary material](#) Fig. 1); ROC curve with the results of the training test of the detector used in the study ([supplementary material](#) Fig. 2); and the example average spectrum computed from a clicks-train of sperm whales echolocation signals ([supplementary material](#) Fig. 3).

ACKNOWLEDGMENTS

This work was supported by the NATO Office of the Chief Scientist under the Climate Change and Security Analysis (OCS000F50) project at CMRE. The NREP22 sea trial has been conducted under the CMRE's Environmental Knowledge and Operational Effectiveness Programme of Work for the NATO Allied Command Transformation. The authors acknowledge the hard work of the NRV Alliance crew and the CMRE and OGS technicians who supported our data collection. This paper represents a contribution from the Projects PNRR-ITINERIS, ICEBERG, and PRIN-ATTRACTION (funded by the Italian Ministry of University and Research, Grant No. 2022CCRN7R). This work is partially supported by EU—Next Generation EU Mission 4 “Education and Research”—Component 2: “From research to business”—Investment 3.1: “Fund for the realisation of an integrated system of research and innovation infrastructures”—Project No. IR0000032—ITINERIS—Italian Integrated Environmental Research Infrastructures System—CUP B53C22002150006.

AUTHOR DECLARATIONS

Conflict of Interest

The authors declare they have no conflicts of interest to disclose.

Ethics Approval

The research presented in this paper is about non-human vertebrate animals in their natural environment. Our data were collected using passive acoustics as a tool to remotely sense the presence of animals without having any contact with the animals.

DATA AVAILABILITY

Data and software supporting this research are restricted by government policies. Data and software are available in the CMRE servers, with access restricted only to

governmental institutions of NATO member Nations and are not accessible to the public or research community. Should the need arise, the data set and software could be disclosed upon viable request via the establishment of a non-disclosure agreement. A formal request for the disclosure of the data can be addressed to NATO CMRE contact point via the official website <https://www.cmre.nato.int/>.

- Adler-Fenchel, H. S. (1980). "Acoustically derived estimate of the size distribution for a sample of sperm whales (*Physeter catodon*) in the western North Atlantic," *Can. J. Fish. Aquat. Sci.* **37**, 2358–2361.
- Ahonen, H., Stafford, K. M., Lydersen, C., Berchok, C. L., Moore, S. E., and Kovacs, K. M. (2021). "Interannual variability in acoustic detection of blue and fin whale calls in the Northeast Atlantic High Arctic between 2008 and 2018," *Endang. Species Res.* **45**, 209–224.
- Ainslie, M. A., and McColm, J. G. (1998). "A simplified formula for viscous and chemical absorption in sea water," *J. Acoust. Soc. Am.* **103**(3), 1671–1672.
- Backus, R. H., and Schevill, W. E. (1966). "Physeter clicks," in *Whales, Dolphins, and Porpoises*, edited by K. S. Norris (University of California Press, Berkeley, CA), pp. 510–528.
- Barber, D. G., Haakon, H., Mundy, C. J., Else, B., Dmitrenko, I. A., Trenblay, J. E., Ehn, J. K., Assmy, P., Daase, M., Candlish, L. M., and Rysgaard, S. (2015). "Selected physical, biological and biogeochemical implications of a rapidly changing Arctic marginal ice zone," *Prog. Oceanogr.* **139**, 122–150.
- Bengtsson, O., Lydersen, C., and Kovacs, K. M. (2022). "Cetacean spatial trends from 2005 to 2019 in Svalbard, Norway," *Polar Res.* **41**, 7773.
- Bensi, M., Kovačević, V., Langone, L., Aliani, S., Ursella, L., Goszczko, I., Soltwedel, T., Skogseth, R., Nilsen, F., Deponte, D., Mansutti, P., Laterza, R., Rebesco, M., Rui, L., Lucchi, R. G., Wählin, A., Viola, A., Beszczynska-Möller, A., and Rubino, A. (2019). "Deep flow variability offshore South-West Svalbard (Fram Strait)," *Water* **11**(4), 683.
- Bensi, M., Nilsen, F., Ferré, B., Skogseth, R., Moskalik, M., Korhonen, M., Vogedes, D., Kovacevic, V., Paladini de Mendoza, F., Ingrosso, G., Langone, L., Giordano, P., Inall, M., Mano, B., Sundfjord, A., Bailey, A., Foss, Ø., Daase, M., Castro de la Guardia, L., Divya, D. T., Renner, A., Dumont, E., Glowacki, O., Ogg, F., Olsen, H., Dølvén, K. O., and Jones, E. (2025). "The Atlantification process in Svalbard: A broad view from the SIOS marine infrastructure network," in *SESS Report 2024* (Svalbard Integrated Arctic Earth Observing System, Longyearbyen, Norway), pp. 138–151.
- Berzin, A. A. (1972). *Kashalot (The Sperm Whale)* (Pischevaya Promyshlennost, Moscow, Russia).
- Best, P. B. (1979). "Social organisation in sperm whales, *Physeter macrocephalus*," in *Behavior of Marine Mammals*, edited by H. E. Winn and B. L. Olla (Springer, New York), pp. 227–289.
- Best, P. B., Canham, P. A. S., and Macleod, N. (1984). "Patterns of reproduction in sperm whales, *Physeter macrocephalus*," *Rep. Int. Whal. Comm.* **5**, 51–79.
- Bivand, R. (2023). *Spatial Data Science: With Applications in R* (Chapman and Hall, London, UK).
- Bjørke, H. (2001). "Predators of the squid *Gonatus fabricii* (Lichtenstein) in the Norwegian Sea," *Fish. Res.* **52**, 113–120.
- Böttcher, A., Gero, S., Beedholm, K., Whitehead, H., and Madsen, P. T. (2018). "Variability of the inter-pulse interval in sperm whale clicks with implications for size estimation and individual identification," *J. Acoust. Soc. Am.* **144**(1), 365–374.
- Caruso, F., Sciacca, V., Bellia, G., De Domenico, E., Larosa, G., Papale, E., Pellegrino, C., Pulvirenti, S., Riccobene, G., Simeone, F., Speziale, F., Viola, S., and Pavan, G. (2015). "Size distribution of sperm whales acoustically identified during long term deep-sea monitoring in the Ionian Sea," *PLoS One* **10**, e0144503.
- Christensen, I. (1980). "Observations of large whales (minke not included) in the North Atlantic 1976–78 and markings of fin, sperm and humpback whales in 1978," *Rep. Int. Whal. Comm.* **30**, 205–208.
- Christensen, I., Haug, T., and Oien, N. (1992). "Seasonal distribution, exploitation and present abundance of stocks of large baleen whales (Mysticeti) and sperm whales (*Physeter macrocephalus*) in Norwegian and adjacent waters," *ICES J. Mar. Sci.* **49**, 341–355.
- Clarke, M. R. (1978). "Structure and proportions of the spermaceti organ in the sperm whale," *J. Mar. Biol. Assoc. UK* **58**, 1–17.
- Clarke, M. R. (1980). "Cephalopoda in the diet of sperm whales of the Southern Hemisphere and their bearing on sperm whale biology" (Institute of Oceanographic Sciences, Surrey, UK).
- Clarke, M. R., and MacLeod, N. (1976). "Cephalopod remains from sperm whales caught off Iceland," *J. Mar. Biol. Assoc.* **56**, 733–750.
- Clarke, M. R., Martins, H. R., and Pascoe, P. (1993). "The diet of sperm whales *Physeter macrocephalus* Linnaeus 1758 off the Azores," *Philos. Trans. R. Soc. London, Ser. B: Biol. Sci.* **339**, 67–82.
- Clarke, R., Paliza, O., and Aguayo, A. (1988). "Sperm whales of the south-east pacific, part IV: Fatness, food and feeding," in *Investigations on Cetacea*, edited by G. Pilleri (University of Berne, Berne, Switzerland), Vol. XXI, pp. 53–195.
- Coakes, A., and Whitehead, H. (2004). "Social structure and mating system of sperm whales off northern Chile," *Can. J. Zool.* **82**, 1360–1369.
- Connor, R. C., Mann, J., Tyack, P. L., and Whitehead, H. (1998). "Social evolution in toothed whales," *Trends Ecol. Evol.* **13**(6), 228–232.
- Davidson, E. (2016). "Exploring the characteristics of spatial distribution for sperm whales (*Physeter macrocephalus*) and northern bottlenose whales (*Hyperoodon ampullatus*) in the arctic: A preliminary study to inform conservation management," Ph.D. thesis, University Akureyri, Akureyri, Iceland.
- Davidson, E. R., Ferguson, S. H., Higdon, J. W., and Treble, M. A. (2023). "Opportunistic sightings from fisheries surveys inform habitat suitability for northern bottlenose whales *Hyperoodon ampullatus* and sperm whales *Physeter macrocephalus* in Baffin Bay and Davis Strait, Canadian Arctic," *Mar. Ecol. Prog. Ser.* **723**, 57–71.
- Davis, G. E., Baumgartner, M. F., Corkeron, P. J., Bell, J., Berchok, C., Bonnell, J. M., Thornton, J. B., Brault, S., Buchanan, G. A., Cholewiak, D. M., Clark, C. W., Delarue, J., Hatch, L. T., Klinck, H., Kraus, S. D., Martin, B., Mellinger, D. K., Moors-Murphy, H., Nieuwkirk, S., Nowacek, D. P., Parks, S. E., Parry, D., Pegg, N., Read, A. J., Rice, A. N., Risch, D., Scott, A., Soldevilla, M. S., Stafford, K. M., Stanistreet, J. E., Summers, E., Todd, S., and Van Parijs, S. M. (2020). "Exploring movement patterns and changing distributions of baleen whales in the western North Atlantic using a decade of passive acoustic data," *Glob. Change Biol.* **26**, 4812–4840.
- Davis, J., and Goadrich, M. (2006). "The relationship between precision-recall and ROC curves," in *Proceedings of the 23rd International Conference on Machine Learning*, pp. 233–240.
- Deines, K. (1999). "Backscatter estimation using broadband acoustic doppler current profilers," in *Proceedings of the Sixth Working Conference on Current Measurement*, San Diego, CA, pp. 249–253.
- De Vreese, S., van der Schaar, M., Weissenberger, J., Erbs, F., Kosecka, M., Solé, M., and André, M. (2018). "Marine mammal acoustic detections in the Greenland and Barents Sea, 2013–2014 seasons," *Sci. Rep.* **8**, 16882.
- Dunnington, D. (2023). "ggspatial: Spatial Data Framework for ggplot2," <https://github.com/paleolimbot/ggspatial> (Last viewed August 19, 2025).
- Eguiguren, A., Konrad, C. M., and Cantor, M. (2023). "Sperm whale reproductive strategies: Current knowledge and future directions," in *Sex in Cetaceans*, edited by B. Würsig and D. N. Orbach (Springer, New York).
- Evans, P. G. H. (1997). "Ecology of sperm whales (*Physeter macrocephalus*) in the Eastern North Atlantic, with special reference to sightings & strandings records from the British Isles," *Bull. Inst. R. Sci. Nat. Belg.* **67**, 37–46.
- Fearnbach, H., Durban, J. W., Mizroch, S. A., Barbeaux, S., and Wade, P. R. (2012). "Winter observations of a group of female and immature sperm whales in the high-latitude waters near the Aleutian Islands, Alaska," *Mar. Biodivers. Rec.* **5**, e13.
- Fisher, F. H., and Simmons, V. P. (1977). "Sound absorption in sea water," *J. Acoust. Soc. Am.* **62**(3), 558–565.
- Flanders Marine Institute (2018). IHO Sea Areas, version 3. Available online at <https://www.marinerregions.org>. <https://doi.org/10.14284/323>.
- Frouin-Mouy, H., Kowarski, K., Martin, B., and Bröker, K. (2017). "Seasonal trends in acoustic detection of marine mammals in Baffin Bay and Melville Bay, Northwest Greenland," *Arctic* **70**, 59–76.
- Garroway, C. J., de Greef, E., Lefort, K. J., Thorstensen, M. J., Foote, A. D., Matthews, C. J. D., Higdon, J. W., Kucheravy, C. E., Petersen, S. D., Rosing-Asvid, A., Ugarte, F., Dietz, R., and Ferguson, S. H. (2024). "Climate change introduces threatened killer whale populations and conservation challenges to the Arctic," *Glob. Change Biol.* **30**, e17352.

- Gero, S., Milligan, M., Rinaldi, C., Francis, P., Gordon, J., Carlson, C., Steffen, A., Tyack, P., Evans, P., and Whitehead, H. (2014). "Behavior and social structure of the sperm whales of Dominica, West Indies," *Mar Mam Sci* **30**, 905–922.
- Giorli, G., and Goetz, K. T. (2019). "Foraging activity of sperm whales (*Physeter macrocephalus*) off the East Coast of New Zealand," *Sci. Rep.* **9**(1), 12182.
- Giorli, G., and Goetz, K. T. (2020). "Acoustically estimated size distribution of sperm whales (*Physeter macrocephalus*) off the East Coast of New Zealand," *N. Z. J. Mar. Freshw. Res.* **54**(2), 177–188.
- Giorli, G., and Pinkerton, M. H. (2019). "Long-term soundscape monitoring in the Ross Sea and its marine protected area," *Proc. Mtgs. Acoust.* **37**(1), 070013.
- Giorli, G., and Pinkerton, M. H. (2023). "Sperm whales forage year-round in the ross sea region," *Front. Remote Sens.* **4**, 940627.
- Goold, J. C., Bennell, J. D., and Jones, S. E. (1996). "Sound velocity measurements in spermaceti oil under the combined influences of temperature and pressure," *Deep-Sea Res. I: Oceanogr. Res. Pap* **43**(7), 961–969.
- Goold, J. C., and Jones, S. E. (1995). "Time and frequency domain characteristics of sperm whale clicks," *J. Acoust. Soc. Am.* **98**(3), 1279–1291.
- Gordon, J. C. D. (1987). "The behaviour and ecology of sperm whales off Sri Lanka," Ph.D. thesis, University of Cambridge, Cambridge, UK.
- Gordon, J. C. D. (1991). "Evaluation of a method for determining the length of sperm whales (*Physeter catodon*) from their vocalizations," *J. Zool.* **224**, 301–314.
- Growcott, A., Miller, B., Sirguey, P., Slooten, E., and Dawson, S. (2011). "Measuring body length of male sperm whales from their clicks: The relationship between inter-pulse intervals and photogrammetrically measured lengths," *J. Acoust. Soc. Am.* **130**, 568–573.
- Guerra, D., Schroeder, K., Borghini, M., Camatti, E., Pansera, M., Schroeder, A., Sparnocchia, S., and Chiggiato, J. (2019). "Zooplankton diel vertical migration in the Corsica Channel (north-western Mediterranean Sea) detected by a moored acoustic Doppler current profiler," *Ocean Sci.* **15**(3), 631–649.
- Hamilton, C. D., Lydersen, C., Aars, J., Acquarone, M., Atwood, T., Baylis, A., Biuw, M., Boltunov, A. N., Born, E. W., Boveng, P., Brown, T. M., Cameron, M., Citta, J., Crawford, J., Dietz, R., Elias, J., Ferguson, S. H., Fisk, A., Folkow, L. P., Frost, K. J., Glazov, D. M., Granquist, S. M., Gryba, R., Harwood, L., Haug, T., Heide-Jørgensen, M. P., Hussey, N. E., Kalinec, J., Laidre, K. L., Litovka, D. I., London, J. M., Loseto, L. L., Macphee, S., Marcoux, M., Matthews, C. J. D., Nilssen, K., Nordøy, E. S., O’Corry-Crowe, G., Øien, N., Olsen, M. T., Quakenbush, L., Rosing-Asvid, A., Semenova, V., Sheldon, K. E. W., Shpak, O. V., Stenson, G., Storrie, L., Sveegard, S., Teilmann, J., Ugarte, F., Von Duyke, A. L., Watt, C., Wiig, Ø., Wilson, R. R., Yurkowski, D. J., and Kovacs, K. M. (2022). "Marine mammal hotspots across the circumpolar Arctic," *Divers. Distrib.* **28**, 2729–2753.
- Hansen, R. G., Boye, T. K., Larsen, R. S., Nielsen, N. H., Tervo, O., Nielsen, R. D., Rasmussen, M. H., Sinding, M. H. S., and Heide-Jørgensen, M. P. (2019). "Abundance of whales in west and east Greenland in summer 2015," *NAMMCO Sci. Pub.* **11**, 1–17.
- Irvine, L., Palacios, D. M., Urbán, J., and Mate, B. (2017). "Sperm whale dive behavior characteristics derived from intermediate-duration archival tag data," *Ecol. Evol.* **7**, 7822–7837.
- Jansen, T., Post, S., Kristiansen, T., Øskarsson, G. J., Boje, J., MacKenzie, B. R., Broberg, M., and Siegstad, H. (2016). "Ocean warming expands habitat of a rich natural resource and benefits a national economy," *Ecol. Appl.* **26**, 2021–2032.
- Jaquet, N. (1996). "How spatial and temporal scales influence understanding of sperm whale distribution: A review," *Mammal Rev.* **26**, 51–65.
- Jaquet, N., Dawson, S., and Douglas, L. (2001). "Vocal behavior of male sperm whales: Why do they click?," *J. Acoust. Soc. Am.* **109**, 2254–2259.
- Kawakami, T. (1980). "A review of sperm whale food," *Sci. Rep. Whales Res. Inst.* **32**, 199–218.
- Kinsler, L. E., Frey, A. R., Coppens, A. B., and Sanders, J. V. (2000). *Fundamentals of Acoustics*, 4th ed. (Wiley, New York).
- Klinck, H., Nieukirk, S. L., Mellinger, D. K., Klinck, K., Matsumoto, H., and Dziak, R. P. (2012). "Seasonal presence of cetaceans and ambient noise levels in polar waters of the North Atlantic," *J. Acoust. Soc. Am.* **132**, EL176–EL181.
- Kobayashi, H., Whitehead, H., and Amano, M. (2020). "Long-term associations among male sperm whales (*Physeter macrocephalus*)," *PLoS One* **15**(12), e0244204.
- Kovacs, K. M., Lydersen, C., Stafford, K., and Wiig, Ø. (2015). "Passive tools for monitoring endangered species in Svalbard: Monitoring the distribution and relative abundance of red listed whales (Project 12/29)," <https://www.miljovernfondet.no/wp-content/uploads/2020/02/12-29-passive-tools-for-monitoring-endangered-species-in-svalbard.pdf> (Last viewed August 19, 2025).
- Lefort, K. J., Garroway, C. J., and Ferguson, S. H. (2020). "Killer whale abundance and predicted narwhal consumption in the Canadian Arctic," *Glob Change Biol.* **26**, 4276–4283.
- Lind, S., Ingvaldsen, R. B., and Furevik, T. (2018). "Arctic warming hot-spot in the northern Barents Sea linked to declining sea-ice import," *Nat. Clim. Change* **8**, 634–639.
- Liu, Y., Guo, J., Xue, Y., Sangmanee, C., Wang, H., Zhao, C., Khokiattiwong, S., and Yu, W. (2022). "Seasonal variation in diel vertical migration of zooplankton and micronekton in the Andaman Sea observed by a moored ADCP," *Deep Sea Res. I* **179**, 103663.
- Long, Z., Perrie, W., Zhang, M., and Liu, Y. (2024). "Responses of Atlantic water inflow through Fram Strait to Arctic storms," *Geophys. Res. Lett.* **51**, e2023GL107777, <https://doi.org/10.1029/2023GL107777>.
- Madsen, P. T., Wahlberg, M., and Møhl, B. (2002). "Male sperm whale (*Physeter macrocephalus*) acoustics in a high-latitude habitat: Implications for echolocation and communication," *Behav. Ecol. Sociobiol.* **53**, 31–41.
- Martin, A. R., and Clarke, M. R. (1986). "The diet of sperm whales (*Physeter macrocephalus*) captured between Iceland and Greenland," *J. Mar. Biol. Assoc.* **66**, 779–790.
- Miller, B. S., and Miller, E. J. (2018). "The seasonal occupancy and diel behaviour of Antarctic sperm whales revealed by acoustic monitoring," *Sci. Rep.* **8**(1), 5429.
- Miller, P. J. O., Johnson, M. P., and Tyack, P. L. (2004). "Sperm whale behaviour indicates the use of echolocation click buzzes "creaks" in prey capture," *Proc. R. Soc. London B.* **271**, 2239–2247.
- Mizroch, S. A., and Rice, D. W. (2013). "Ocean nomads: Distribution and movements of sperm whales in the North Pacific shown by whaling data and Discovery marks," *Mar. Mammal Sci.* **29**, E136–E165.
- Møhl, B. (2001). "Sound transmission in the nose of the sperm whale *Physeter catodon*. A post mortem study," *J. Comp. Physiol. A* **187**, 335–340.
- Møhl, B., and Amundin, M. (1991). "Sperm whale clicks: Pulse interval in clicks from a 21 m specimen," in *Sound production in odontocetes, with emphasis on the harbour porpoise, *Phocoena phocoena**, Ph.D. thesis, University of Stockholm, Stockholm, Sweden, p. 115–125.
- Møhl, B., Larsen, E., and Amundin, M. (1981). "Sperm whale size determination: Outlines of an acoustic approach," *FAO Fish. Ser.* **5**, 327–332.
- Møhl, B., Wahlberg, M., Madsen, P. T., Heerfordt, A., and Lund, A. (2003). "The monopleural nature of sperm whale clicks," *J. Acoust. Soc. Am.* **114**, 1143–1154.
- Møhl, B., Wahlberg, M., Madsen, P. T., Miller, L. A., and Surlykke, A. (2000). "Sperm whale clicks: Directionality and source level revisited," *J. Acoust. Soc. Am.* **107**, 638–648.
- Mullison, J. (2017). "Backscatter Estimation using Broadband Acoustic Doppler Current Profilers – Updated," Application Note No. FSA-031 (Teledyne Analytical Instruments, City of Industry, CA).
- Nieukirk, S. L., Mellinger, D. K., Dziak, R. P., Matsumoto, H., and Klinck, H. (2020). "Multi-year occurrence of sei whale calls in North Atlantic polar waters," *J. Acoust. Soc. Am.* **147**(3), 1842–1850.
- Nishiwaki, N., Ohsumi, S., and Maeda, Y. (1963). "Change of form in the sperm whale accompanied with growth," *Sci. Rep. Whale Res. Inst. Tokyo* **17**, 1–13.
- Norris, K. S., and Harvey, G. W. (1972). "A theory for the function of the spermaceti organ of the sperm whale (*Physeter macrocephalus*)," in *Animal Orientation and Navigation*, edited by S. R. Galler, K. Schmidt-Koenig, G. J. Jacobs, and R. E. Belleville (NASA, Washington, DC), pp. 397–419.
- O’Callaghan, S. A., Griffin, B., Levesque, S., Gammell, M., and O’Brien, J. (2024). "Female, juvenile, and calf sperm whale *Physeter macrocephalus* (Linnaeus 1758) records from Ireland," *Ecol. Evol.* **14**, e70056.
- Oestreich, W. K., Benoit-Bird, K. J., Abrahms, B., Margolina, T., Joseph, J. E., Zhang, Y., Rueda, C. A., and Ryan, J. P. (2024). "Evidence for seasonal migration by a cryptic top predator of the deep sea," *Move. Ecol.* **12**, 65.
- Ohsumi, S. (1966). "Sexual segregation of the sperm whale in the North Pacific," *Sci. Rep. Whales Res. Inst. Tokyo* **20**, 1–16.

- Øien, N. (2009). "Distribution and abundance of large whales in Norwegian and adjacent waters based on ship surveys 1995–2001," *NAMMCO Sci. Pub.* **7**, 31–47.
- Øynes, P. (1957). "Om spermhvalen" ("About the sperm whale"), *Fauna (Oslo)* **10**, 125–132.
- Pavan, G., Hayward, T. J., Borsani, J. F., Priano, M., Manghi, M., Fossati, C., and Gordon, J. (2000). "Time patterns of sperm whale codas recorded in the Mediterranean Sea 1985–1996," *J. Acoust. Soc. Am.* **107**, 3487–3495.
- Pebesma, E. (2018). "Simple features for R: Standardized support for spatial vector data," *R J.* **10**(1), 439–446.
- Polyakov, I. V., Alkire, M. B., Bluhm, B. A., Brown, K., Carmack, E. C., Chierici, M., Danielson, S., Ellingsen, I., Ershova, E. A., Gärdfeldt, K., Ingvaldsen, R. B., Pnyushkov, A. V., Slagstad, D., and Wassman, P. (2020). "Borealization of the Arctic Ocean in response to anomalous advection from sub-arctic seas," *Front. Mar. Sci.* **7**, 491.
- Posdajjian, N., Soderstjerna, C., Jones, J. M., Solsona-Berga, A., Hildebrand, J. A., Westdal, K., Ootoowak, A., and Baumann-Pickering, S. (2022). "Changes in sea ice and range expansion of sperm whales in the eclipse sound region of Baffin Bay, Canada," *Glob. Change Biol.* **28**, 3860–3870.
- Posdajjian, N., Solsona-Berga, A., Hildebrand, J. A., Soderstjerna, C., Wiggins, S. M., Lenssen, K., and Baumann-Pickering, S. (2024). "Sperm whale demographics in the Gulf of Alaska and Bering Sea/Aleutian Islands: An overlooked female habitat," *PLoS One* **19**(7), e0285068.
- Powers, D. M. (2020). "Evaluation: From precision, recall and F-measure to ROC, informedness, markedness and correlation," *arXiv:2010.16061*.
- Pöyhönen, V., Thomisch, K., Kovacs, K. M., Lydersen, C., and Ahonen, H. (2024). "High Arctic 'hotspots' for sperm whales (*Physeter macrocephalus*) off western and northern Svalbard, Norway, revealed by multi-year passive acoustic monitoring (PAM)," *Sci. Rep.* **14**, 5825.
- Rantanen, M., Karpechko, A. Y., Lippinen, A., Nordling, K., Hyvärinen, O., Ruostenoja, K., Vihma, T., and Laaksonen, A. (2022). "The Arctic has warmed nearly four times faster than the globe since 1979," *Commun. Earth Environ.* **3**, 168.
- R Core Team (2024). "R: A language and environment for statistical computing," <https://www.R-project.org/> (Last viewed August 19, 2025).
- Reichel, G., and Nachtnebel, H. P. (1994). "Suspended sediment monitoring in a fluvial environment: Advantages and limitations applying an acoustic Doppler current profiler," *Water Res.* **28**(4), 751–761, [https://doi.org/10.1016/0043-1354\(94\)90083-3](https://doi.org/10.1016/0043-1354(94)90083-3).
- Rice, D. W. (1989). "Sperm whale *Physeter macrocephalus* linnaeus, 1758," in *Handbook of Marine Mammals*, edited by S. H. Ridgway and R. Harrison (Academic Press, San Diego, CA), Vol. 4, pp. 177–233.
- Rødland, E. S., and Bjørge, A. (2015). "Residency and abundance of sperm whales (*Physeter macrocephalus*) in the Bleik Canyon, Norway," *Mar. Biol. Res.* **11**(9), 974–982.
- Santos, M. B., Pierce, G. J., Boyle, P. R., Reid, R. J., Ross, H. M., Patterson, I. A. P., Kinze, C. C., Tougaard, S., Lick, R., Piatkowski, U., and Hernández-García, V. (1999). "Stomach contents of sperm whales *Physeter macrocephalus* stranded in the North Sea 1990–1996," *Mar. Ecol. Prog. Ser.* **183**, 281–294.
- Schwertman, N. C., Owens, M. A., and Adnan, R. (2004). "A simple more general kernel boxplot method for identifying outliers," *Comput. Stat. Data Anal.* **47**(1), 165–174.
- Seeger, K. D., and Miksis-Olds, J. L. (2020). "A decade of marine mammal acoustical presence and habitat preference in the Bering Sea," *Polar Biol.* **43**, 1549–1569.
- Simon, M., Stafford, K. M., Beedholm, K., Lee, C. M., and Madsen, P. T. (2010). "Singing behavior of fin whales in the Davis Strait with implications for mating, migration and foraging," *J. Acoust. Soc. Am.* **128**(5), 3200–3210.
- Skarsoulis, E. K., Piperakis, G. S., Orfanakis, E., Papadakis, P., Pavlidi, D., Kalogerakis, M. A., Alexiadou, P., and Frantzis, A. (2022). "A real-time acoustic observatory for sperm-whale localization in the eastern Mediterranean Sea," *Front. Mar. Sci.* **9**, 873888.
- Snøeijjs-Leijonmalm, P., Flores, H., Sakinan, S., Hildebrandt, N., Svenson, A., Castellani, G., Vane, K., Mark, F. C., Heuzé, C., Tippenhauer, S., Niehoff, B., Hjeltn, J., Sundberg, J. H., Schaafsma, F. L., Engelmann, R., and The Efica-Mosaic Team (2022). "Unexpected fish and squid in the central Arctic deep scattering layer," *Sci. Adv.* **8**, eabj7536.
- Solsona-Berga, A., Posdajjian, N., Hildebrand, J. A., and Baumann-Pickering, S. (2022). "Echolocation repetition rate as a proxy to monitor population structure and dynamics of sperm whales," *Remote Sens. Ecol. Conserv.* **8**, 827–840.
- Spielhagen, R. F., Werner, K., Sørensen, S. A., Zamelczyk, K., Kandiano, E., Budeus, G., Husum, K., Marchitto, T. M., and Hald, M. (2011). "Enhanced modern heat transfer to the arctic by warm Atlantic water," *Science* **331**, 450–453.
- Stevens, B. (2022). "Acoustic absorption in seawater," <https://www.mathworks.com/matlabcentral/fileexchange/28653-acoustic-absorption-in-seawater> (Last viewed August 19, 2025).
- Storrie, L., Lydersen, C., Andersen, M., Wynn, R. B., and Kovacs, K. M. (2018). "Determining the species assemblage and habitat use of cetaceans in the Svalbard Archipelago, based on observations from 2002 to 2014," *Polar Res.* **37**, 1463065.
- Teigen, S. H., Nilsen, F., Skogseth, R., Gjevik, B., and Beszczynska-Möller, A. (2011). "Baroclinic instability in the West Spitsbergen Current," *J. Geophys. Res.* **116**, C07012, <https://doi.org/10.1029/2011JC006974>.
- Teloni, V., Johnson, M. P., Miller, P. J. O., and Madsen, P. T. (2008). "Shallow food for deep divers: Dynamic foraging behavior of male sperm whales in a high latitude habitat," *J. Exp. Mar. Biol. Ecol.* **354**(1), 119–131.
- Teloni, V., Zimmer, W. M. X., Wahlberg, M., and Madsen, P. T. (2007). "Consistent acoustic size estimation of sperm whales using clicks recorded from unknown aspects," *J. Cetac. Res. Manage.* **9**(2), 127–136.
- Tverberg, V., Nøst, O. A., Lydersen, C., and Kovacs, K. M. (2014). "Winter sea ice melting in the Atlantic Water subduction area, Svalbard Norway," *JGR Oceans* **119**, 5945–5967.
- Ursella, L., Cardin, V., Batistić, M., Garić, R., and Gačić, M. (2018). "Evidence of zooplankton vertical migration from continuous Southern Adriatic buoy current-meter records," *Prog. Oceanogr.* **167**, 78–96.
- Vacquié-Garcia, J., Lydersen, C., Marques, T. A., Ahonen, H., Skern-Mauritzen, M., Øien, N., and Kovacs, K. M. (2017). "Late summer distribution and abundance of ice-associated whales in the Norwegian High Arctic," *Endang. Species Res.* **32**, 59–70.
- Vihtakari, M. (2024). "ggOceanMaps: Plot data on oceanographic maps using ggplot2. R package version 2.2.0," <https://mikkovihtakari.github.io/ggOceanMaps/> (Last viewed August 19, 2025).
- Ward, J. A., Thomas, L., Jarvis, S., DiMarzio, N., Moretti, D., Marques, T. A., Marques, T. A., Dunn, C., Laridge, D. C., and Hartvig, E. (2012). "Passive acoustic density estimation of sperm whales in the Tongue of the Ocean, Bahamas," *Mar. Mammal Sci.* **28**(4), E444–E455.
- Wassmann, P., Duarte, C. M., Agustí, S., and Sejr, M. K. (2011). "Footprints of climate change in the Arctic marine ecosystem," *Glob. Change Biol.* **17**, 1235–1249.
- Watkins, W. A. (1980). "Acoustics and the behavior of sperm whales," in *Animal Sonar Systems*. NATO Advanced Study Institutes Series Vol. 28, edited by R. G. Busnel and J. F. Fish (Springer, Boston, MA).
- Watkins, W. A., and Schevill, W. E. (1977). "Sperm whale codas," *J. Acoust. Soc. Am.* **62**, 1485–1490.
- Watwood, S. L., Miller, P. J. O., Johnson, M., Madsen, P. T., and Tyack, P. L. (2006). "Deep-diving foraging behaviour of sperm whales (*Physeter macrocephalus*)," *J. Anim. Ecol.* **75**, 814–825.
- Weilgart, L., and Whitehead, H. (1988). "Distinctive vocalizations from mature male sperm whales (*Physeter macrocephalus*)," *Can. J. Zool.* **66**, 1931–1937.
- Weir, C. R., Pollock, C., Cronin, C., and Taylor, S. (2001). "Cetaceans of the Atlantic Frontier, north and west of Scotland," *Cont. Shelf Res.* **21**, 1047–1071.
- Whitehead, H. (1993). "The behavior of mature male sperm whales on the Galapagos Islands breeding grounds," *Can. J. Zool.* **71**, 689–699.
- Whitehead, H. (1994). "Delayed competitive breeding in roving males," *J. Theor. Biol.* **166**(2), 127–133.
- Whitehead, H. (2018). "Sperm whale: *Physeter microcephalus*," in *Encyclopedia of Marine Mammals*, edited by B. Würsig (Elsevier, Amsterdam, the Netherlands), pp. 919–925.
- Whitehead, H. (2003). *Sperm Whales: Social Evolution in the Ocean* (University of Chicago Press, Chicago, IL).
- Whitehead, H., and Weilgart, L. (1991). "Patterns of visually observable behaviour and vocalizations in groups of female sperm whales," *Behaviour* **118**(3/4), 275–296.
- Wickham, H. (2016). *ggplot2: Elegant Graphics for Data Analysis* (Springer-Verlag, New York).

Zimmer, W. M. X., Johnson, M. P., D'Amico, A., and Tyack, P. L. (2003). "Combining data from a multisensor tag and passive sonar to determine the diving behavior of a sperm whale (*Physeter macrocephalus*)," *IEEE J. Oceanic Eng.* **28**, 13–28.

Zimmer, W. M. X., Madsen, P. T., Teloni, V., Johnson, M. P., and Tyack, P. L. (2005a). "Off-axis effects on the multi-pulse structure of sperm

whale usual clicks with implications for sound production," *J. Acoust. Soc. Am.* **118**(5), 3337–3345.

Zimmer, W. M. X., Tyack, P. L., Johnson, M. P., and Madsen, P. T. (2005b). "Three-dimensional beam pattern of regular sperm whale clicks confirms bent-horn hypothesis," *J. Acoust. Soc. Am.* **117**(3), 1473–1485.